A 250-YEAR PERIODICITY IN SOUTHERN HEMISPHERE WESTERLY WINDS OVER THE LAST 2600 YEARS

Affiliations: Chris S.M. Turney[1,2*], Richard T. Jones[3], Christopher Fogwill[1,2], Jackie Hatton[3], Alan N. Williams[4,5], Alan Hogg[6], Zoë Thomas[1,2], Jonathan Palmer[1,2], Scott Mooney[1], and Ron W. Reimer[7]

1. School of Biological, Earth and Environmental Sciences, University of New South Wales, Sydney, Australia

2. Climate Change Research Centre, School of Biological, Earth and Environmental Sciences, University of New South Wales, Sydney, Australia

3. Department of Geography, Exeter University, Devon, EX4 4RJ, United Kingdom

4. Fenner School of Environment and Society, The Australian National University, Canberra, ACT 0200, Australia

5. Archaeological & Heritage Management Solutions Pty Ltd, 2/729 Elizabeth Street, Waterloo, NSW 2017, Australia

6. Waikato Radiocarbon Laboratory, University of Waikato, Private Bag 3105, Hamilton, New Zealand

7. School of Geography, Archaeology and Palaeoecology, Queen's University Belfast. Belfast BT7 1NN, U.K.

* E-mail: c.turney@unsw.edu.au

Abstract

Southern Hemisphere westerly airflow has a significant influence on the ocean-atmosphere system of the mid- to high-latitudes with potentially global climate implications. Unfortunately historic observations only extend back to the late nineteenth century, limiting our understanding of multi-decadal to centennial change. Here we present a highly resolved (30-year) record of past westerly wind strength from a Falkland Islands peat sequence spanning the last 2600 years. Situated within the core latitude of Southern Hemisphere westerly airflow, we identify highly variable changes in exotic pollen and charcoal derived from South America which can be used to inform on past westerly air strength. We find a period of high charcoal content between 2000 and 1000 cal. yrs BP, associated with increased burning in Patagonia, most probably as a result of higher temperatures and stronger westerly airflow. Spectral analysis of the charcoal record identifies a pervasive c.250-year periodicity that is coherent with radiocarbon production rates suggesting solar variability has a modulating influence on Southern Hemisphere westerly airflow with important implications for understanding global climate change through the late Holocene.

Keywords: Falkland Islands; exotic pollen; radiocarbon (^{14}C) dating; solar forcing; Southern Annular Mode (SAM); Southern Hemisphere Westerlies

1. Introduction

A major limitation for quantifying the magnitude and impact of change across the Southern Ocean is the relatively short duration or low resolution of ocean-atmosphere records. This is particularly significant with regards to the Southern Hemisphere westerly storm belt, which since the mid-1970s, has undergone a significant intensification and southward shift (Gillett et al., 2008; Messié and Chavez, 2011). One measure of this change in atmospheric circulation is the Southern Annular Mode (SAM), described as the pressure difference between Antarctica (65˚S) and the latitude band at around 40°S (Karpechko et al., 2009; Marshall, 2003). Since the mid-1970s, SAM appears to have undergone a positive shift in the troposphere, which has been associated with hemispheric-wide changes in the atmosphere-ocean-ice domains, including precipitation patterns and significant surface and subsurface ocean warming (Cook et al., 2010; Delworth and Zeng, 2014; Domack et al., 2005; Gille, 2008, 2014; Thompson et al., 2011). This trend is projected to continue during the 21st century as a result of both ongoing greenhouse gas emissions and a persistence of the Antarctic ozone hole (Liu and Curry, 2010; Thompson et al., 2011; Yin, 2005), potentially resulting in reduced Southern Ocean uptake of anthropogenic CO_2 (Ito et al., 2010; Le Quére et al., 2009; Lenton et al., 2013; Marshall, 2003; Marshall and Speer, 2012).

While no observational records for SAM extend beyond the late nineteenth century (Fogt et al., 2009; Marshall, 2003; Visbeck, 2009), proxy records of past westerly airflow have been generated on annual to centennial timescales through the Holocene (Abram et al., 2014; Björck et al., 2012; Lamy et al., 2010; Lisé-Pronovost et al., 2015; McGlone et al., 2010; Strother et al., 2015; Villalba et al., 2012). Crucially the

association between proxies and changes in westerly wind strength and/or latitude is often implied but few provide a direct measure of past airflow or directly test their interpretation through time. One possibility is the identification of exotic airborne particles preserved in sedimentary sequences. Ideally, the peat or lake record should be close enough to the source to have a relatively high input of material (e.g. pollen, charcoal) but not so close that the influx is constant over time. Whilst numerous studies have been undertaken in the Arctic (Fredskild, 1984; Jessen et al., 2011) and the high-latitudes of the Indian and Pacific oceans (McGlone et al., 2000; Scott and van Zinderen Barker, 1985), few have been reported from the south Atlantic. Recent work on a lake core taken from Annekov Island, South Georgia (Strother et al., 2015) demonstrates the considerable potential of this approach but the relatively large distance from the nearest source in South America (Figure 1) (approximately 2100 km) limits the delivery of pollen with no charcoal reported.

Here we report a new high-resolution record of westerly airflow over the past 2600 years from the Falkland Islands. The Falkland Islands (52˚S) lie within the main latitudinal belt of Southern Hemisphere westerly airflow, 500 to 730 km east of Argentina and 1410 km west of Annekov Island. The close proximity to South America means that these islands receive a relatively high input of particles from the continental mainland (Barrow, 1978; Rose et al., 2012), making them an ideal location to investigate past changes in westerly airflow.

2. Methods

The Falkland Islands are a low-lying archipelago in the South Atlantic Ocean, situated in the furious fifties wind belt on the southeast South American

continental shelf at 51-52˚S, 58-61˚W (Figure 1). The Falkland Islands experience a cool temperate but relatively dry oceanic climate, dominated by westerly winds (Otley et al. 2008). Across the year, the temperature ranges from 2.2˚C (July) to 9˚C (February), with the islands experiencing a relatively low but variable precipitation (typically ranging between 500 and 800 mm/year) lying in the lee of the Andes. Modern climate records show the prevailing wind direction across the Falkland Islands is predominantly from the west with strong winds throughout the year and no significant seasonal variation (Upton and Shaw, 2002).

Climate amelioration following the Last Glacial Maximum led to the establishment of blanket peat across large parts of the islands from 16,500 cal. years BP (Wilson et al., 2002). To investigate past westerly airflow in the late Holocene, an exposed Ericaceous-grass peatland was cored on Canopus Hill, above Port Stanley Airport (51.691˚S, 57.785˚W, approximately 30 m above sea level) (Figure 1). The one-metre sequence reported here comprises a uniform dark-brown peat from which the uppermost 90 cm was contiguously sampled for pollen, charcoal and comprehensive dating.

Pollen samples were prepared using standard palynological techniques (Faegri and Iverson, 1975). Volumetric samples were taken every 1 cm along the core and *Lycopodium* spores were added as a 'spike'. The samples were deflocculated with hot 10 % NaOH and then sieved through a 106 µm mesh. The samples then underwent acetolysis, to remove extraneous organic matter before the samples were mounted in silicon oil. Pollen types/palynomorphs were counted at 400 X

magnification until a minimum of 300 target grains were identified. The pollen counts were expressed as percentages, with only terrestrial land pollen (TLP) contributing to the final pollen sum. Pollen/palynomorphs were identified using standard pollen keys (Barrow, 1978; Macphail and Cantrill, 2006) and the pollen type slide collection at Exeter University. Past fire activity was assessed using micro-charcoal counts of fragments (<106μm) identified on the pollen slides (Whitlock and Larsen, 2001). Counts were undertaken at each level until a fixed total of 50 lycopodium spores were counted and the total expressed as a concentration (fragments per cm^3). More than 99% of charcoal fragments were less than 50μm in size, with negligible amounts identified in the 50-106μm and >106μm fractions.

Terrestrial plant macrofossils (fruits and leaves) were extracted from the peat sequence and given an acid-base-acid (ABA) pretreatment and then combusted and graphitized in the University of Waikato AMS laboratory, with $^{14}C/^{12}C$ measurement by the University of California at Irvine (UCI) on a NEC compact (1.5SDH) AMS system. The pretreated samples were converted to CO_2 by combustion in sealed pre-baked quartz tubes, containing Cu and Ag wire. The CO_2 was then converted to graphite using H_2 and an Fe catalyst, and loaded into aluminum target holders for measurement at UCI. This was supplemented by ^{137}Cs measurements down the profile to detect the onset of nuclear tests. ^{137}Cs analysis was undertaken following standard techniques with measurements made using an ORTEC high- resolution, low-background coaxial germanium detectors. Detectable measurements were obtained between 8.5 and 9.5 cm and

assigned an age of CE 1963, the time of early radionuclide fallout at these latitudes (Hancock et al., 2011).

The radiocarbon and ^{137}Cs ages were used to develop an age model using a `P_sequence` deposition model in OxCal 4.2 (Ramsey, 2008) with `General Outlier` analysis detection (probability=0.05) (Ramsey, 2011). The ^{14}C ages were calibrated against the Southern Hemisphere calibration (SHCal13) dataset . Using Bayes theorem, the algorithms employed sample possible solutions with a probability that is the product of the prior and likelihood probabilities. Taking into account the deposition model and the actual age measurements, the posterior probability densities quantify the most likely age distributions; the outlier option was used to detect ages that fall outside the calibration model for each group, and if necessary, down-weight their contribution to the final age estimates. Modelled ages are reported here as thousands of calendar years BP or cal. BP (Table 1 and Figure 2). The pollen sequence reported here spans the last 2600 yrs with an average 30-year resolution (Figure 3).

To investigate the periodicities preserved in the palaeoenvironmental proxies utilised herein, we undertook Multi-Taper Method (MTM) analysis using a narrowband signal, red noise significance and robust noise background estimation (with a resolution of 2 and 3 tapers) (Thomson, 1982). We also applied single spectrum analysis (SSA), which applies an empirical orthogonal function (EOF) analysis to the autovariance matrix on the chronologies. Here we undertook a Monte Carlo significance test (95% significance), using a window of 9, a Burg covariance, and 8 components. Both analyses used the software

125 *kSpectra* version 3.4.3 (3.4.5). Wavelet analysis was undertaken on the 30-year
126 averaged charcoal data using the R package 'biwavelet' (Gouhier, 2013). The
127 Morlet continuous wavelet transform was applied, and the data were padded
128 with zeros at each end to reduce wraparound effects (Torrence and Webster,
129 1999). To test the robustness of the obtained periodicities, the Lomb-Scargle
130 algorithm was employed, a spectral decomposition method that computes the
131 spectral properties of time series with irregular sampling intervals (Ruf, 1999),
132 in this instance, the 'raw' charcoal values. This method minimises bias and
133 induced periodicities that may arise from interpolating missing or unevenly
134 spaced data. The technique was undertaken using the `lsp()` function within the
135 `'lomb'` package in R (v.3.0.2). Periodicities were extracted from data sets using
136 Analyseries (Paillard et al., 1996).
137
138 A measure of solar variability was derived by calculating the ^{14}C production rate
139 using the IntCal13 atmospheric radiocarbon dataset (Reimer et al., 2013) and an
140 ocean–atmosphere box diffusion model (Oeschger et al., 1975); the same as that
141 reported in previous studies (Bond et al., 2001; Turney et al., 2005). The model
142 consists of one box for the atmosphere, one for the ocean mixed layer, 37 boxes
143 for the thermocline, five boxes for the deep ocean and two for the biosphere
144 (short and long residence time) (Stuiver and Braziunas, 1993a). The climate-
145 influenced mixing parameters (air-gas sea exchange, eddy diffusivity, and
146 biospheric uptake and release) were held constant through the run using the
147 same setup as Marine04 (Table 2) (Hughen et al., 2004). The model was
148 parameterized to produce a pre-industrial marine mixed layer ^{14}C of -46.5 ‰

149 and a deep ocean value of -190‰ at CE 1830 for the 2013 marine calibration
150 dataset Marine13 (Reimer et al., 2013).
151
152 **3. Results and Discussion**
153 Only a limited number of Holocene pollen records have been reported from the
154 Falkland Islands (Barrow, 1978). The pollen record in the uppermost 90 cm at
155 Canopus Hill is dominated by *Poaceae* and *Empetrum,* consistent with previous
156 work and today's vegetation (Barrow, 1978; Broughton and McAdam, 2003;
157 Clark et al., 1998). The most significant change in the pollen taxa is a pronounced
158 shift to increased representation of *Asteroideae* (accompanied by a relative
159 decline in *Poaceae*) centered on 47 cm (equivalent to 1100 cal. BP) (Figure 2).
160 Although undifferentiated in the counts, the *Asteroideae* are most likely
161 *Chilliotrichum diffusum*, common on the island across a range of habitats
162 including *Empetrum* heath (Broughton and McAdam, 2003). The shift in the
163 pollen diagram therefore most likely reflects the replacement of upland
164 grasslands by *Empetrum* heath. Highly variable charcoal counts were obtained
165 through the sequence (<106 μm) (Figure 2), with negligible macrocharcoal
166 fragments (>106μm) identified, suggesting there was little or no fire on the site.
167
168 The exotic pollen taxa were expressed as concentration values to explore their
169 changing input onto the site over the last 2600 yrs (Figure 2). Although this data
170 could be re-expressed as a pollen influx, the interpretation of flux data in non-
171 annually laminated sequences can be strongly influenced by the choice of age
172 model and the density of dated points down the core (Davis, 1969; Hicks and
173 Hyvärinen, 1999). Consideration of the radiocarbon and ^{137}Cs ages (Table 1)

174 suggests that the depth-age relationship can be described by a linear relationship
175 (r^2 = 0.98) below a depth of 18 cm (Figure 3). This means that the pollen (and
176 charcoal) concentration data below this depth are equivalent to influx. In the
177 uppermost section of the core (above 18 cm) a faster rate of sediment
178 accumulation (or less compaction) means that the deposition time is reduced.
179
180 Importantly, the sequence preserves a record of exotic pollen delivery into the
181 site, with *Nothofagus* dominating the input but with trace amounts of *Podocarp*,
182 *Ephedra fragilis* and *Anacardium*-type record (<0.5% total land pollen), all
183 originating from South America. Whilst the low levels of most exotic pollen
184 precludes meaningful interpretation, all samples contain *Nothofagus* (<5% total
185 land pollen), a taxa not known to have grown on the Falkland Islands since the
186 Middle Miocene/Early Pliocene (Macphail and Cantrill, 2006) but has been
187 detected in Lateglacial (Clark et al., 1998) and Holocene (Barrow, 1978)
188 sequences. Producing relatively small pollen grains (20-40μm in diameter)
189 (Wang et al., 2000), the nearest source of contemporary *Nothofagus* is South
190 America which extends from 33˚ in central Chile to 56˚S on Tierra del Fuego
191 (Veblen et al., 1996). The youngest arboreal macrofossils of the other exotic taxa
192 are dated to late Tertiary deposits on West Point Island, West Falkland (Birnie
193 and Roberts, 1986).
194
195 Whilst exotic pollen values are relatively low, peaks in *Nothofagus* coincide with
196 increased amounts of charcoal in the Canopus Hill sequence. Importantly,
197 negligible amounts of macro-charcoal (>106μm) were identified, suggesting the
198 charcoal has been blown to the site from Patagonia. The aerial delivery of the

charcoal to the Falkland Islands is supported by the close correspondence with charcoal in Laguna Guanaco in southwest Patagonia (51˚S) (Moreno et al., 2009). Importantly, *Nothofagus* dominates lowland Patagonian vegetation and, in areas away from human activity, was established by 5000 cal. years BP (Iglesias et al., 2014; Kilian and Lamy, 2012), with a stepped expansion in *Nothofagus* at Laguna Guanaco centred on 570 BP (Moreno et al., 2009) and evidence for temporary forest fragmentation during periods of stronger westerly airflow (Moreno et al., 2014). In marked contrast to Patagonia, the Falklands *Nothofagus* pollen record is highly variable and of sufficient concentration to recognize similar changes to those in the charcoal record, with periods of high fire frequency associated with high input of exotic pollen.

Although charcoal fragments <106μm might reflect fire in the local environment, charcoal of this size can be transported long distances (Clark, 1988). The vast majority of the charcoal fragments <50 μm, comparable in size to exotic *Nothofagus* (20-40μm) and *Podocarpus* (40-50μm in diameter) pollen (Wang et al., 2000; Wilson and Owens, 1999). The close correspondence between the *Nothofagus* pollen record and charcoal fragments in the Canopus Hill sequence on the Falkland Islands strongly suggests similar sources, indicating the higher charcoal counts provides a more robust measure of the westerly airflow. A sustained period of charcoal delivery to the Falkland Islands is observed between 2000 and 1000 cal. BP, with prominent peaks in *Nothofagus* and charcoal recognized at approximately 2400, 2100, 1800-1300, 1000, 550 and 250 cal. BP (Figure 2) which we interpret here as stronger westerly wind flow.. Our results suggest reports of pre-European human activity on the Falkland

Islands as inferred by the presence of charcoal in peat sequences (Buckland and Edwards, 1998) may be premature.

In contrast to previous work at Annenkov Island which suggested enhanced westerly airflow is associated with wetter conditions (Strother et al., 2015), we observe the reverse. Modern comparisons between the SAM (as a measure of westerly airflow) (Marshall, 2003) and air temperature suggest a positive correlation (Abram et al., 2014). Comparing historic observations of SAM with ERA79 Interim reanalysis (Dee et al., 2011), we observe a highly significant relationship with more positive phases of SAM associated with warmer 2-10 metre height air temperatures and wind speeds across much of South America, the Antarctic Peninsula and the Falkland Islands (Figure 4), supporting our interpretation. The contrasting moisture interpretation to that in South Georgia may be a result of the rain shadow effect of the Andes on the Falklands. It should be noted, however, that the reanalysis product used here is only for the period commencing CE 1979 (the satellite era) and that different atmospheric dynamics may have been involved in the delivery of exotic pollen and charcoal to the Falkland Islands on centennial timescales.

The MTM analysis identifies two different periodicities in the charcoal record (<106μm) from Canopus Hill significant above 95%: 242 and 95 yrs, with the former exhibiting a broad multi-decadal peak (Figure 5A). To test whether the MTM spectral peak is robust, we undertook SSA on the sequence chronologies. A Monte Carlo significance test identified a significant periodicity (above 95%) at 231 yrs (Figure 5B). Furthermore, the Lomb-Scargle algorithm identified a 268-

249 yr peak (Figure 5C), indicating this periodicity is pervasive through the record
250 regardless of the sampling method, and therefore robust.
251
252 The existence of a 200-250 yr periodicity has been identified in numerous
253 Holocene records globally (Galloway et al., 2013; Poore et al., 2004), including
254 Southern Ocean productivity as recorded in Palmer Deep (Domack et al., 2001;
255 Leventer et al., 1996) and dust deposition over Antarctica (Delmonte et al.,
256 2005). Furthermore, whilst no spectral analysis was undertaken, a series of
257 recurring 200-yr long dry/warm periods have recently been reported from
258 Patagonia over the last three millennia and linked to positive SAM-like
259 conditions (Moreno et al., 2014). The origin of the ~250 yr periodicity may be
260 linked to postulated centennial-scale changes in climate modes of variability
261 including the El Niño-Southern Oscillation (ENSO) (Ault et al., 2013) or Southern
262 Ocean convection (Martin et al., 2013). Importantly, a 200-250 yr periodicity has
263 also been observed in records of atmospheric ^{14}C and ^{10}Be (Adolphi et al., 2014;
264 Steinhilber et al., 2012; Stuiver and Braziunas, 1993b; Turney et al., 2005),
265 suggesting the so-called de Vries solar cycle may play a role (Leventer et al.,
266 1996).
267
268 The detection of solar forcing in palaeo records is highly sensitive to the
269 chronological framework being investigated (Gray et al., 2010). To explore the
270 possible role of solar variability on Southern Hemisphere westerly airflow we
271 first analyzed the modelled production rate of ^{14}C derived from 5-yr resolved
272 tree-ring data (Reimer et al., 2013), a cosmogenic radionuclide that is produced
273 in the upper atmosphere (with ^{14}C increasing with reduced solar activity) (Bond

et al., 2001; Turney et al., 2005). We resampled the ^{14}C dataset at 30-yr resolution to mimic the resolution of the Canopus Hill sequence and compared these to the Total Solar Irradiance (TSI) generated from the polar ice core ^{10}Be which is reported at a 20-30 yr resolution (Steinhilber et al., 2009) (Figure 6). Regardless of the dataset used, the same pattern is observed with large amplitude changes in solar irradiance between 2600 and 2300 years ago and from 1300 cal. years BP to present day, but with sustained high irradiance between 2300 and 1300 cal. years BP (Figure 6A, C and E). We find the 5-year resolved IntCal13 dataset produces a periodicity comparable to the Falkland Islands record (225 yrs at 99% confidence; Figure 6A and B). Importantly, when we look at the downscaled records of solar irradiance, the statistical significance decreases in the lower-resolved ^{14}C dataset (230 yrs at 90%; Figure 6C and D) or shifts to a lower frequency in the ^{10}Be record (202 yrs at 99%; Figure 6E and F).

Our results imply that the central Southern Hemisphere westerlies were particularly strong during 2000 and 1000 cal. BP and/or lay close to the latitude of the Falkland Islands, at least within the South American sector (Figure 7). Records of comparable latitude and age from South America are Laguna Guanaco (51˚S) (Moreno et al., 2014) and Palm2 (53˚S) (Lamy et al., 2010). The Laguna Guanaco record captures a remarkably similar fire history as preserved in the Canopus Hill with a pronounced peak in charcoal over the same period (Figure 7D). In Palm2, accumulation rates of biogenic carbonate provide a proxy for salinity changes in surface fjord waters off the west coast of Chile with lower salinities associated with strong winds and relatively high precipitation, limiting

299 the influence of the open ocean water and reducing biogenic carbonate
300 production. While the dataset from Palm2 does not have the resolution of the
301 other records, a similar trend with pervasive lower salinities (stronger westerly
302 winds) is recorded between 2000 and 1000 cal. yrs BP (Figure 7E). Whilst the
303 change in the trend may be interpreted as reflecting either a change in the
304 latitude and/or strength of the winds, the parallel peaks and troughs in
305 *Nothofagus* and charcoal from Canopus Hill (in contrast to constant *Nothofagus*
306 levels at Laguna Guanaco – (Moreno et al., 2009)) imply the core latitude of the
307 westerly winds has not changed and instead was particularly strong between
308 2000 and 1000 cal. yrs BP, resulting in increased fire frequency in Patagonia
309 (Holz and Veblen, 2012). This is supported by a study on Patagonian *Fitzroya*
310 *cupressoides* from 40-42˚S (Roig et al., 2001). Whilst a living series spanning
311 1,229-yrs did not identify a 200-250 yr periodicity, a 245 yr cycle was identified
312 in a floating 50,000 yr-old tree ring series of comparable length, consistent with
313 our record suggesting a suppression of this periodicity across a large latitudinal
314 range over the last 1000 years. Importantly, the ~250-yr periodicity identified in
315 the charcoal record varies in amplitude over the last 2600 yrs (Figures 7A-C). A
316 Gaussian filtered curve and wavelet plot shows the ~250 year periodicity is most
317 strongly expressed between 2600 and 1000 cal. BP, and spans the prominent
318 (sustained) peak in charcoal, with an implied reduction in the expression of the
319 ~250 year periodicity over the last millennium.
320
321 The role changing solar output may have on westerly airflow is not immediately
322 apparent. The period of strongest inferred winds falls within a millennial-
323 duration period of high solar irradiance (Figure 7F) but with a relatively muted

250-yr periodicity in the 5-yr resolved ^{14}C production rate data (Figure 7G). We do, however, observe a consistent relationship, with peaks in solar irradiance leading charcoal on the order of 20-40 years, suggesting Southern Hemisphere westerly winds may be particularly sensitive to the de Vries cycle during periods of high solar irradiance and less sensitive with reduced solar output. How solar periodicity may influence the strength of Southern Hemisphere westerly airflow is not precisely known. One possibility is that the ~250 yr periodicity may change salinity in the North Atlantic (Stuiver and Braziunas, 1993b), driving changes in the Meridional Overturning Circulation that are transmitted globally. However, the existence of the same periodicity in the delivery of dust on to the East Antarctic Ice Sheet (Delmonte et al., 2005) does imply a direct atmospheric link, either through changing sea ice extent or sea surface temperatures, or via the westerlies themselves (Shindell et al., 1999). Recent work has highlight the role of high solar irradiance in increasing troposphere-stratosphere coupling, extending the seasonal length during which stronger Southern Hemisphere westerly winds are experienced at the surface (Kuroda and Yamazaki, 2010), similar to that observed in the Northern Hemisphere (Ineson et al., 2011). Alternatively, recent modelling work suggests insolation changes can lead to increased 'baroclinicity' (Fogwill et al., 2015) or a 'Split Jet' (Chiang et al., 2014), strengthening westerly winds. Further work is required to understand the driving mechanism(s) behind the ~250 yr periodicity on global climate.

4. Conclusions

Southern Hemisphere westerly airflow is believed to play a significant role in precipitation, sea ice extent, sea surface temperatures and the carbon cycle

across the mid to high latitudes. Unfortunately, the observational record only extends back to the late nineteenth century, limiting our understanding of what drives past changes in westerly winds. Although proxies of westerly airflow can provide long-term perspectives on past change, few provide a direct (passive) measure of westerly winds. Exotic pollen and charcoal fragments sourced upwind of sedimentary sequences can potentially provide a valuable insight into past variability. Here we report a new, comprehensively-dated high-resolution pollen record from a peat sequence on the Falkland Islands which lies under the present core of Southern Hemisphere westerly airflow (the so-called 'furious fifties') and spanning the last 2600 years. We observe peaks in taxa from South America (particularly *Nothofagus*) and charcoal fragments (<106μm) that appear to be linked to warm and windy conditions. Spectral analysis identifies a robust ~250-yr periodicity, with evidence of stronger westerly airflow between 2000 and 1000 cal. yrs BP. In comparison with other Southern Hemisphere records, the 250-yr periodicity suggests solar forcing plays a role in modulating the strength of the Southern Hemisphere westerlies, something hitherto not recognised, and will form the focus of future research.

Acknowledgements

CSMT and CF acknowledge the support of the Australian Research Council (FL100100195, FT120100004 and DP130104156). We thank the Falkland Islands Government for permission to undertake sampling on the island (permit number: R07/2011) and Darren Christie for assisting with the fieldwork. Many

thanks to Joel Pedro and an anonymous reviewer for their insightful and constructive comments. The data are lodged on the NOAA Paleoclimate Archive.

Competing financial interests

The authors declare no competing financial interests.

References

Abram, N. J., Mulvaney, R., Vimeux, F., Phipps, S. J., Turner, J., and England, M. H.: Evolution of the Southern Annular Mode during the past millennium, Nature Climate Change, 4, 564-569, 2014.

Adolphi, F., Muscheler, R., Svensson, A., Aldahan, A., Possnert, G., Beer, J., Sjolte, J., Bjorck, S., Matthes, K., and Thieblemont, R.: Persistent link between solar activity and Greenland climate during the Last Glacial Maximum, Nature Geoscience, 7, 662-666, 2014.

Ault, T. R., Deser, C., Newman, M., and Emile-Geay, J.: Characterizing decadal to centennial variability in the equatorial Pacific during the last millennium, Geophysical Research Letters, 40, 3450-3456, 2013.

Barrow, C.: Postglacial pollen diagrams from south Georgia (sub-Antarctic) and West Falkland island (South Atlantic), Journal of Biogeography, 5, 251-274, 1978.

Birnie, J. F. and Roberts, D. E.: Evidence of Tertiary forest in the Falkland Islands (Ilas Malvinas), Palaeogeography, Palaeoclimatology, Palaeoecology, 55, 45-53, 1986.

Björck, S., Rundgren, M., Ljung, K., Unkel, I., and Wallin, Å.: Multi-proxy analyses of a peat bog on Isla de los Estados, easternmost Tierra del Fuego: a unique record of the variable Southern Hemisphere Westerlies since the last deglaciation, Quaternary Science Reviews, 42, 1-14, 2012.

Bond, G., Kromer, B., Beer, J., Muscheler, R., Evans, M. N., Showers, W., Hoffman, S., Lotti-Bond, R., Hajdas, I., and Bonani, G.: Persistent solar influence on North Atlantic climate during the Holocene, Science, 294, 2130-2136, 2001.

Bronk Ramsey, C. and Lee, S.: Recent and planned developments of the program OxCal, Radiocarbon, 55, 720-730, 2013.

Broughton, D. A. and McAdam, J. H.: The current status and distribution of the Falkland Islands pteridophyte flora, Fern Gazette, 17, 21-38, 2003.

Buckland, P. C. and Edwards, K. J.: Palaeoecological evidence for possible Pre-European settlement in the Falkland Islands, Journal of Archaeological Science, 25, 599-602, 1998.

Chiang, J. C., Lee, S.-Y., Putnam, A. E., and Wang, X.: South Pacific Split Jet, ITCZ shifts, and atmospheric North–South linkages during abrupt climate changes of the last glacial period, Earth and Planetary Science Letters, 406, 233-246, 2014.

Clark, J. S.: Particle motion and the theory of charcoal analysis: source area, transport, deposition, and sampling, Quaternary Research, 30, 67-80, 1988.

Clark, R., Huber, U. M., and Wilson, P.: Late Pleistocene sediments and environmental change at Plaza Creek, Falkland Islands, South Atlantic, Journal of Quaternary Science, 13, 95-105, 1998.

Cook, A. J., Poncet, S., Cooper, A. P. R., Herbert, D. J., and Christie, D.: Glacier retreat on South Georgia and implications for the spread of rats, Antarctic Science, 22, 255-263, 2010.

421 Davis, M. B.: Climatic changes in southern Connecticut recorded by pollen
422 deposition at Rogers Lake, Ecology, 50, 409-422, 1969.

423 Dee, D. P., Uppala, S. M., Simmons, A. J., Berrisford, P., Poli, P., Kobayashi, S.,
424 Andrae, U., Balmaseda, M. A., Balsamo, G., Bauer, P., Bechtold, P., Beljaars, A. C. M.,
425 van de Berg, L., Bidlot, J., Bormann, N., Delsol, C., Dragani, R., Fuentes, M., Geer, A.
426 J., Haimberger, L., Healy, S. B., Hersbach, H., Hólm, E. V., Isaksen, L., Kållberg, P.,
427 Köhler, M., Matricardi, M., McNally, A. P., Monge-Sanz, B. M., Morcrette, J. J., Park,
428 B. K., Peubey, C., de Rosnay, P., Tavolato, C., Thépaut, J. N., and Vitart, F.: The ERA-
429 Interim reanalysis: configuration and performance of the data assimilation
430 system, Quarterly Journal of the Royal Meteorological Society, 137, 553-597,
431 2011.

432 Delmonte, B., Petit, J., Krinner, G., Maggi, V., Jouzel, J., and Udisti, R.: Ice core
433 evidence for secular variability and 200-year dipolar oscillations in atmospheric
434 circulation over East Antarctica during the Holocene, Climate Dynamics, 24, 641-
435 654, 2005.

436 Delworth, T. L. and Zeng, F.: Regional rainfall decline in Australia attributed to
437 anthropogenic greenhouse gases and ozone levels, Nature Geosci, 7, 583-587,
438 2014.

439 Domack, E., Duran, D., Leventer, A., Ishman, S., Doane, S., McCallum, S., Amblas, D.,
440 Ring, J., Gilbert, R., and Prentice, M.: Stability of the Larsen B ice shelf on the
441 Antarctic Peninsula during the Holocene epoch, Nature, 436, 681-685, 2005.

442 Domack, E., Leventer, A., Dunbar, R., Taylor, F., Brachfeld, S., and Sjunneskog, C.:
443 Chronology of the Palmer Deep site, Antarctic Peninsula: a Holocene

444 palaeoenvironmental reference for the circum-Antarctic, The Holocene, 11, 1-9,
445 2001.

446 Faegri, K. and Iverson, J.: Textbook of pollen analysis, Blackwell, Oxford, 1975.

447 Fogt, R. L., Perlwitz, J., Monaghan, A. J., Bromwich, D. H., Jones, J. M., and Marshall,
448 G. J.: Historical SAM variability. Part II: Twentieth-Century variability and trends
449 from reconstructions, observations, and the IPCC AR4 models, Journal of Climate,
450 22, 5346-5365, 2009.

451 Fogwill, C. J., Turney, C. S. M., Hutchinson, D. K., Taschetto, A. S., and England, M.
452 H.: Obliquity control on Southern Hemisphere climate during the Last Glacial,
453 Nature Scientific Reports, 5, 2015.

454 Fredskild, B.: Holocene palaeo-winds and climatic changes in West Greenland as
455 indicated by long-distance transported and local pollen in lake sediments. In:
456 Climatic Changes on a Yearly to Millennial Basis, Mörner, N. A. and Karlén, W.
457 (Eds.), Springer Netherlands, Dordrecht, The Netherlands, 1984.

458 Galloway, J. M., Wigston, A., Patterson, R. T., Swindles, G. T., Reinhardt, E., and
459 Roe, H. M.: Climate change and decadal to centennial-scale periodicities recorded
460 in a late Holocene NE Pacific marine record: Examining the role of solar forcing,
461 Palaeogeography, Palaeoclimatology, Palaeoecology, 386, 669-689, 2013.

462 Gille, S. T.: Decadal-scale temperature trends in the Southern Hemisphere ocean,
463 Journal of Climate, 21, 4749-4765, 2008.

464 Gille, S. T.: Meridional displacement of the Antarctic Circumpolar Current,
465 Philosophical Transactions of the Royal Society A: Mathematical, Physical and
466 Engineering Sciences, 372, 2014.

467 Gillett, N. P., Stone, D. A., Stott, P. A., Nozawa, T., Karpechko, A. Y., Hegerl, G. C.,
468 Wehner, M. F., and Jones, P. D.: Attribution of polar warming to human influence,
469 Nature Geoscience, 1, 750-754, 2008.

470 Gouhier, T.: biwavelet: Conduct univariate and bivariate wavelet analyses
471 (Version 0.14)
472 . 2013.

473 Gray, L. J., Beer, J., Geller, M., Haigh, J. D., Lockwood, M., Matthes, K., Cubasch, U.,
474 Fleitmann, D., Harrison, G., Hood, L., Luterbacher, J., Meehl, G. A., Shindell, D., van
475 Geel, B., and White, W.: Solar influences on climate, Reviews of Geophysics, 48,
476 n/a-n/a, 2010.

477 Hancock, G. J., Leslie, C., Everett, S. E., Tims, S. G., Brunskill, G. J., and Haese, R.:
478 Plutonium as a chronomarker in Australian and New Zealand sediments: a
479 comparison with ^{137}Cs, Journal of Environmental Radioactivity, 102, 919-929,
480 2011.

481 Hicks, S. and Hyvärinen, H.: Pollen influx values measured in different
482 sedimentary environments and their palaeoecological implications, Grana, 38,
483 228-242, 1999.

484 Hogg, A. G., Hua, Q., Blackwell, P. G., Niu, M., Buck, C. E., Guilderson, T. P., Heaton,
485 T. J., Palmer, J. G., Reimer, P. J., Reimer, R. W., Turney, C. S. M., and Zimmerman, S.

R. H.: SHCal13 Southern Hemisphere calibration, 0–50,000 years cal BP, Radiocarbon, 55, 1889-1903, 2013.

Holz, A. and Veblen, T. T.: Wildfire activity in rainforests in western Patagonia linked to the Southern Annular Mode, International Journal of Wildland Fire, 21, 114-126, 2012.

Hua, Q. and Barbetti, M.: Review of tropospheric bomb ^{14}C data for carbon cycle modeling and age calibration purposes, Radiocarbon, 2004.

Hughen, K. A., Baillie, M. G., Bard, E., Beck, J. W., Bertrand, C. J., Blackwell, P. G., Buck, C. E., Burr, G. S., Cutler, K. B., and Damon, P. E.: Marine04 marine radiocarbon age calibration, 0-26 cal kyr BP, Radiocarbon, 46, 1059-1086, 2004.

Iglesias, V., Whitlock, C., Markgraf, V., and Bianchi, M. M.: Postglacial history of the Patagonian forest/steppe ecotone (41–43°S), Quaternary Science Reviews, 94, 120-135, 2014.

Ineson, S., Scaife, A. A., Knight, J. R., Manners, J. C., Dunstone, N. J., Gray, L. J., and Haigh, J. D.: Solar forcing of winter climate variability in the Northern Hemisphere, Nature Geoscience, advance online publication, 2011.

Ito, T., Woloszyn, M., and Mazloff, M.: Anthropogenic carbon dioxide transport in the Southern Ocean driven by Ekman flow, Nature, 463, 80-83, 2010.

Jessen, C. A., Solignac, S., Nørgaard-Pedersen, N., Mikkelsen, N., Kuijpers, A., and Seidenkrantz, M.-S.: Exotic pollen as an indicator of variable atmospheric circulation over the Labrador Sea region during the mid to late Holocene, Journal of Quaternary Science, 26, 286-296, 2011.

508 Karpechko, A. Y., Gillett, N. P., Marshall, G. J., and Screen, J. A.: Climate impacts of
509 the Southern Annular Mode simulated by the CMIP3 models, Journal of Climate,
510 22, 3751-3768, 2009.

511 Kilian, R. and Lamy, F.: A review of Glacial and Holocene paleoclimate records
512 from southernmost Patagonia (49–55°S), Quaternary Science Reviews, 53, 1-23,
513 2012.

514 Kuroda, Y. and Yamazaki, K.: Influence of the solar cycle and QBO modulation on
515 the Southern Annular Mode, Geophysical Research Letters, 37, n/a-n/a, 2010.

516 Lamy, F., Kilian, R., Arz, H. W., Francois, J.-P., Kaiser, J., Prange, M., and Steinke, T.:
517 Holocene changes in the position and intensity of the southern westerly wind
518 belt, Nature Geoscience, 3, 695-699, 2010.

519 Le Quére, C., Raupach, M. R., Canadell, J. G., and Marland, G. e. a.: Trends in the
520 sources and sinks of carbon dioxide, Nature Geoscience, 2009. doi:
521 10.1038/ngeo1689, 2009.

522 Lenton, A., Tilbrook, B., Law, R., Bakker, D., Doney, S., Gruber, N., Hoppema, M.,
523 Ishii, M., Lovenduski, N., and Matear, R.: Sea-air CO_2 fluxes in the Southern Ocean
524 for the period 1990–2009, Biogeosciences Discussions, 10, 285-333, 2013.

525 Leventer, A., Domack, E. W., Ishman, S. E., Brachfeld, S., McClennen, C. E., and
526 Manley, P.: Productivity cycles of 200–300 years in the Antarctic Peninsula
527 region: Understanding linkages among the sun, atmosphere, oceans, sea ice, and
528 biota, Geological Society of America Bulletin, 108, 1626-1644, 1996.

529 Lisé-Pronovost, A., St-Onge, G., Gogorza, C., Haberzettl, T., Jouve, G., Francus, P.,
530 Ohlendorf, C., Gebhardt, C., Zolitschka, B., and Team, P. S.: Rock-magnetic proxies
531 of wind intensity and dust since 51,200 cal BP from lacustrine sediments of
532 Laguna Potrok Aike, southeastern Patagonia, Earth and Planetary Science
533 Letters, 411, 72-86, 2015.

534 Liu, J. and Curry, J. A.: Accelerated warming of the Southern Ocean and its
535 impacts on the hydrological cycle and sea ice, Proceedings of the National
536 Academy of Sciences, 107, 14987-14992, 2010.

537 Macphail, M. and Cantrill, D. J.: Age and implications of the Forest Bed, Falkland
538 Islands, southwest Atlantic Ocean: Evidence from fossil pollen and spores,
539 Palaeogeography, Palaeoclimatology, Palaeoecology, 240, 602-629, 2006.

540 Marshall, G.: Trends in the Southern Annular Mode from observations and
541 reanalyses, Journal of Climate, 16, 4134-4143, 2003.

542 Marshall, J. and Speer, K.: Closure of the meridional overturning circulation
543 through Southern Ocean upwelling, Nature Geoscience, 5, 171-180, 2012.

544 Martin, T., Park, W., and Latif, M.: Multi-centennial variability controlled by
545 Southern Ocean convection in the Kiel Climate Model, Climate Dynamics, 40,
546 2005-2022, 2013.

547 McGlone, M., Wilmshurst, J. M., and Wiser, S. K.: Lateglacial and Holocene
548 vegetation and climatic change on Auckland Island, Subantarctic New Zealand,
549 The Holocene, 10, 719-728, 2000.

McGlone, M. S., Turney, C. S. M., Wilmshurst, J. M., and Pahnke, K.: Divergent trends in land and ocean temperature in the Southern Ocean over the past 18,000 years, Nature Geoscience, 3, 622-626, 2010.

Messié, M. and Chavez, F.: Global modes of sea surface temperature variability in relation to regional climate indices, Journal of Climate, 24, 4314-4331, 2011.

Moreno, P., François, J., Villa-Martínez, R., and Moy, C.: Millennial-scale variability in Southern Hemisphere westerly wind activity over the last 5000 years in SW Patagonia, Quaternary Science Reviews, 28, 25-38, 2009.

Moreno, P. I., Vilanova, I., Villa-Martínez, R., Garreaud, R. D., Rojas, M., and De Pol-Holz, R.: Southern Annular Mode-like changes in southwestern Patagonia at centennial timescales over the last three millennia, Nat Commun, 5, 2014.

Oeschger, H., Siegenthaler, U., Schotterrer, U., and Gugelmann, A.: A box diffusion model to study the carbon dioxide exchange in nature, Tellus, 27, 168-192, 1975.

Paillard, D., Labeyrie, L., and Yiou , P.: Macintosh program performs time-series analysis, Eos, 77, 379, 1996.

Poore, R. Z., Quinn, T. M., and Verardo, S.: Century-scale movement of the Atlantic Intertropical Convergence Zone linked to solar variability, Geophysical Research Letters, 31, L12214, 2004.

Ramsey, C. B.: Dealing with outliers and offsets in radiocarbon dating, 2011.

Ramsey, C. B.: Radiocarbon dating: revolutions in understanding, Archaeometry, 50, 249-275, 2008.

Reimer, P. J., Bard, E., Bayliss, A., Beck, J. W., Blackwell, P. G., Bronk Ramsey, C., Grootes, P. M., Guilderson, T. P., Haflidason, H., Hajdas, I., Hatté, C., Heaton, T. J., Hoffmann, D. L., Hogg, A. G., Hughen, K. A., Kaiser, K. F., Kromer, B., Manning, S. W., Niu, M., Reimer, R. W., Richards, D. A., Scott, E. M., Southon, J. R., Staff, R. A., Turney, C. S. M., and van der Plicht, J.: IntCal13 and Marine13 radiocarbon age calibration curves 0–50,000 years cal BP, Radiocarbon, 55, 1869-1887, 2013.

Roig, F. A., Le-Quesne, C., Boninsegna, J. A., Briffa, K. R., Lara, A., Grudd, H., Jones, P. D., and Villagrán, C.: Climate variability 50,000 years ago in mid-latitude Chile as reconstructed from tree rings, Nature, 410, 567-570, 2001.

Rose, N. L., Jones, V. J., Noon, P. E., Hodgson, D. A., Flower, R. J., and Appleby, P. G.: Long-range transport of pollutants to the Falkland Islands and Antarctica: Evidence from lake sediment fly ash particle records, Environmental Science & Technology, 46, 9881-9889, 2012.

Ruf, T.: The Lomb-Scargle periodogram in biological rhythm research: Analysis of incomplete and unequally spaced time-series, Biological Rhythm Research 30, 178-201, 1999.

Scott, L. and van Zinderen Barker, E. M.: Exotic pollen and long-distance wind dispersal at a Sub-Antarctic island, Grana, 24, 45-54, 1985.

Shindell, D., Rind, D., Balachandran, N., Lean, J., and Lonergan, P.: Solar cycle variability, ozone and climate, Science, 284, 305-308, 1999.

Steinhilber, F., Abreu, J. A., Beer, J., Brunner, I., Christl, M., Fischer, H., Heikkilä, U., Kubik, P. W., Mann, M., McCracken, K. G., Miller, H., Miyahara, H., Oerter, H., and

593 Wilhelms, F.: 9,400 years of cosmic radiation and solar activity from ice cores
594 and tree rings, Proceedings of the National Academy of Sciences of the United
595 States of America, 109, 5967-5971, 2012.

596 Steinhilber, F., Beer, J., and Fröhlich, C.: Total solar irradiance during the
597 Holocene, Geophysical Research Letters, 36, L19704, 2009.

598 Strother, S. L., Salzmann, U., Roberts, S. J., Hodgson, D. A., Woodward, J., Van
599 Nieuwenhuyze, W., Verleyen, E., Vyverman, W., and Moreton, S. G.: Changes in
600 Holocene climate and the intensity of Southern Hemisphere Westerly Winds
601 based on a high-resolution palynological record from sub-Antarctic South
602 Georgia, The Holocene, 25, 263-279, 2015.

603 Stuiver, M. and Braziunas, T. F.: Modeling atmospheric C-14 influences and C-14
604 ages of marine samples to 10,000 BC, Radiocarbon, 35, 137-189, 1993a.

605 Stuiver, M. and Braziunas, T. F.: Sun, ocean, climate and atmospheric $^{14}CO_2$: an
606 evaluation of causal and spectral relationships, The Holocene, 3, 289-305, 1993b.

607 Thompson, D. W. J., Solomon, S., Kushner, P. J., England, M. H., Grise, K. M., and
608 Karoly, D. J.: Signatures of the Antarctic ozone hole in Southern Hemisphere
609 surface climate change, Nature Geoscience, 4, 741-749, 2011.

610 Thomson, D. J.: Spectrum estimation and harmonic analysis, Proceedings of the
611 IEEE, 70, 1055–1096, 1982.

612 Torrence, C. and Webster, P. J.: Interdecadal changes in the ENSO–Monsoon
613 system, Journal of Climate, 12, 2679-2690, 1999.

614 Turney, C., Baillie, M., Clemens, S., Brown, D., Palmer, J., Pilcher, J., Reimer, P., and
615 Leuschner, H. H.: Testing solar forcing of pervasive Holocene climate cycles,
616 Journal of Quaternary Science, 20, 511-518, 2005.

617 Upton, J. and Shaw, C. J.: An overview of the oceanography and meteorology of
618 the Falkland Islands, Aquatic Conservation and Freshwater Ecosystems, 12, 15-
619 25, 2002.

620 van Oldenborgh, G. J. and Burgers, G.: Searching for decadal variations in ENSO
621 precipitation teleconnections, Geophysical Research Letters, 32, L15701, 2005.

622 Veblen, T. T., Hill, R. S., and Read, J.: The ecology and biogeography of *Nothofagus*
623 forests, Yale University Press, 1996.

624 Villalba, R., Lara, A., Masiokas, M. H., Urrutia, R., Luckman, B. H., Marshall, G. J.,
625 Mundo, I. A., Christie, D. A., Cook, E. R., Neukom, R., Allen, K., Fenwick, P.,
626 Boninsegna, J. A., Srur, A. M., Morales, M. S., Araneo, D., Palmer, J. G., Cuq, E.,
627 Aravena, J. C., Holz, A., and LeQuesne, C.: Unusual Southern Hemisphere tree
628 growth patterns induced by changes in the Southern Annular Mode, Nature
629 Geoscience, 5, 793-798, 2012.

630 Visbeck, M.: A station-based Southern Annular Mode Index from 1884 to 2005,
631 Journal of Climate, 22, 940-950, 2009.

632 Wang, P.-L., Pu, F.-T., and Zheng, Z.-H.: Pollen morphology of the genus
633 *Nothofagus* and its taxonomic significance, Acta Phytotax. Sinica., 38, 452-461,
634 2000.

635 Whitlock, C. and Larsen, C.: Charcoal as a fire proxy. In: Tracking Environmental
636 Change using Lake Sediments, Springer Netherlands, Dordrecht, The
637 Netherlands, 2001.

638 Wilson, P., Clark, R., Birnie, J., and Moore, D. M.: Late Pleistocene and Holocene
639 landscape evolution and environmental change in the Lake Sulivan area,
640 Falkland Islands, South Atlantic, Quaternary Science Reviews, 21, 1821-1840,
641 2002.

642 Wilson, V. R. and Owens, J. N.: The reproductive biology of Totara (*Podocarpus*
643 *totara*) (Podocarpaceae), Annals of Botany, 83, 401-411, 1999.

644 Yin, J. H.: A consistent poleward shift of the storm tracks in simulations of 21st
645 century climate, Geophysical Research Letters, 32, 2005.

646
647

Table and Figure Captions

Depth, cm	Wk lab number	Material	%M/^{14}C BP ± 1 σ	Modelled years BP ± 1σ
8-9	34598	Fruits and leaves	117.0±0.4%M	-16±11
11-12	32994	Fruits and leaves	107.8±0.4%M	-8±2
18-19	37007	Fruits and leaves	107.3±0.3%M	3±31
25-26	35146	Fruits and leaves	95±25	94±66
35-36	37008	Fruits and leaves	647±25	603±29
39-40	33445	Fruits and leaves	761±25	661±28
57-58	32996	Fruits and leaves	1818±25	1672±51
70-71	32350	Fruits and leaves	2235±25	2201±67
97-98	32997	Fruits and leaves	2749±25	2802±32

Table 1: Radiocarbon and modelled calibrated age ranges using SHCal13 (Hogg et al., 2013) and Bomb04SH (Hua and Barbetti, 2004) using the P_sequence and

Outlier analysis option in OxCal 4.2 (Bronk Ramsey and Lee, 2013; Ramsey, 2008).

Parameter	Marine98	Marine04
Air-gas sea exchange	19 moles/m^2/yr	18.8 moles/m^2/yr
Eddy diffusivity	4000 m^2/yr	4220 m^2/yr
Pre-industrial atmospheric [CO_2]	280 ppm	270 ppm
Initial atmospheric $\Delta^{14}C$	90‰	100‰

Table 2: Box diffusion model parameters for Marine98 (Bond et al., 2001; Turney et al., 2005) versus Marine04 (Hughen et al., 2004).

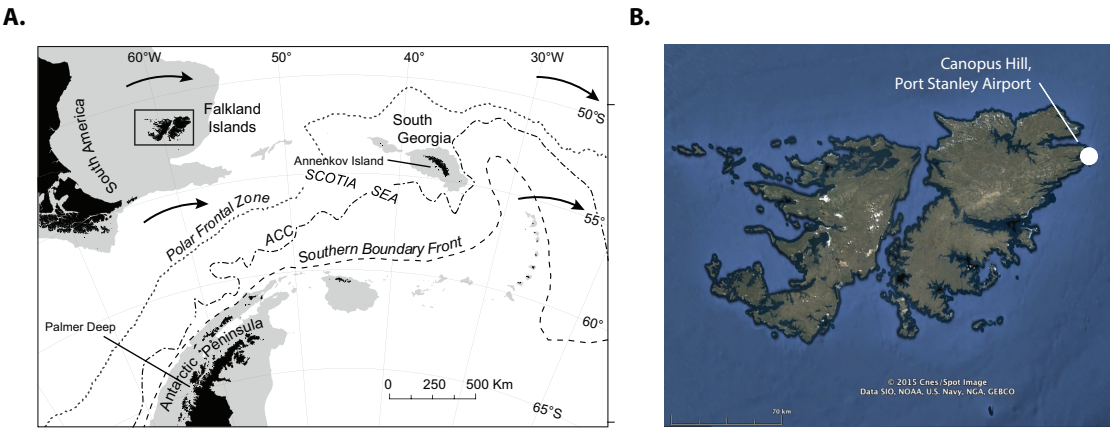

Figure 1: Location of the Falkland Islands in the South Atlantic Ocean with mean locations of the Polar and Southern Boundary fronts (dashed lines), the continental shelf (grey areas) and prevailing westerly airflow (solid arrows) (Panel A); and Canopus Hill, Port Stanley Airport, in the east Falkland Islands (Panel B). Panel 'A' was modified from (Strother et al., 2015) and 'B' was obtained from Google Earth.

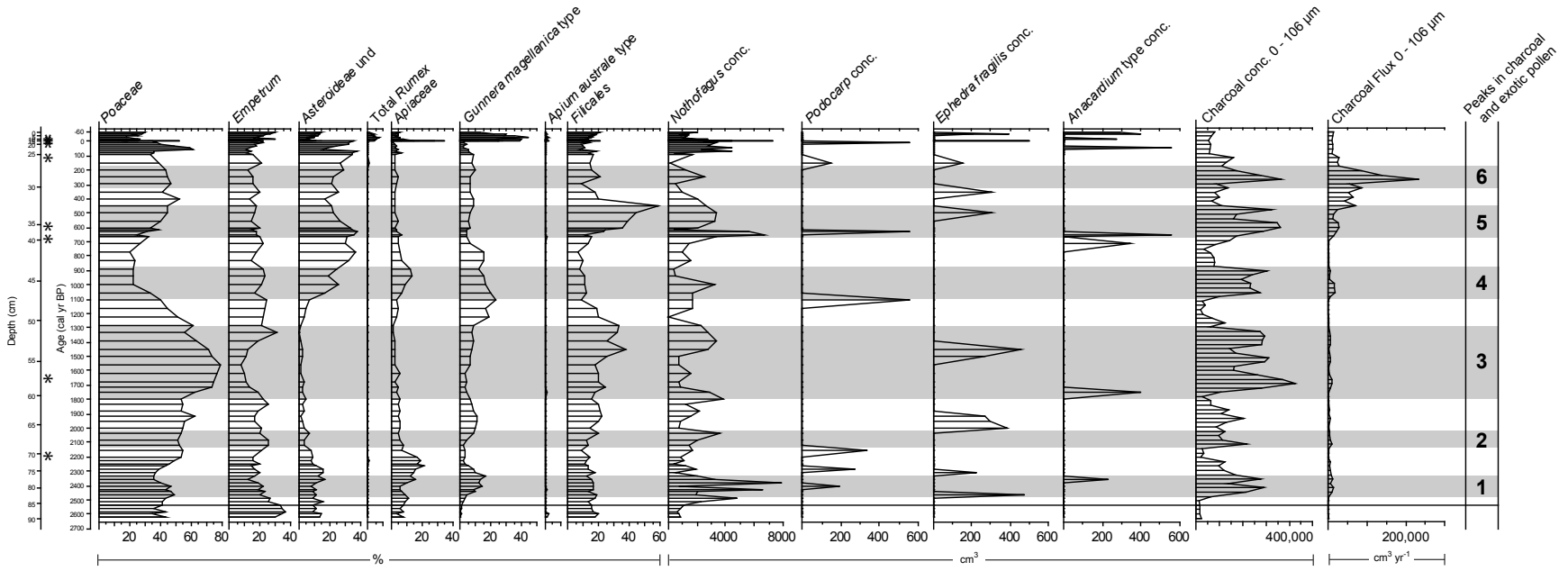

Figure 2: Pollen diagram from Canopus Hill, Port Stanley Airport, plotted against depth and calendar age. The location of ^{137}Cs and ^{14}C ages are marked by asterisk.

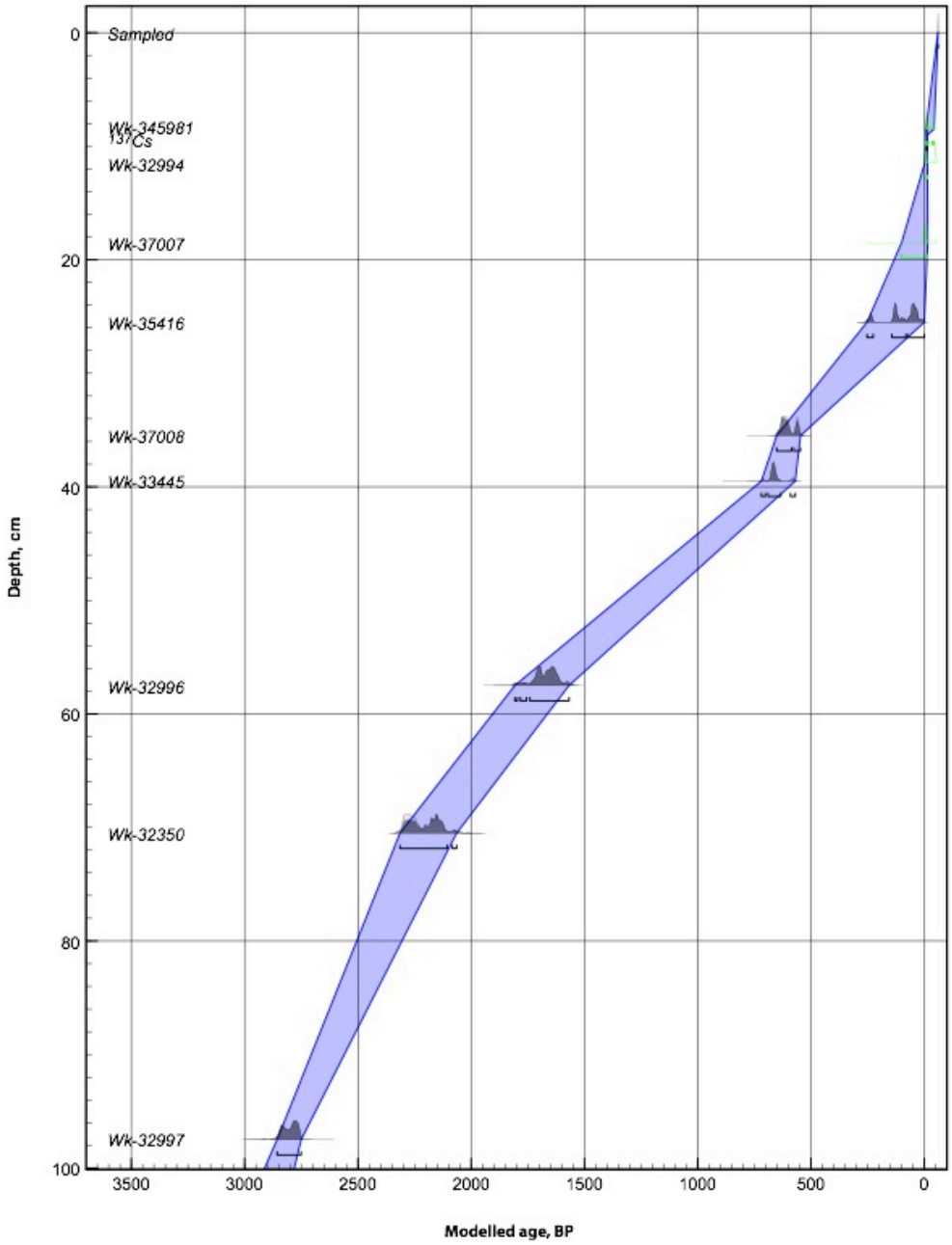

Figure 3: Age-depth plot for Canopus Hill, Port Stanley Airport, with 1σ age range (blue envelope) and probability distributions.

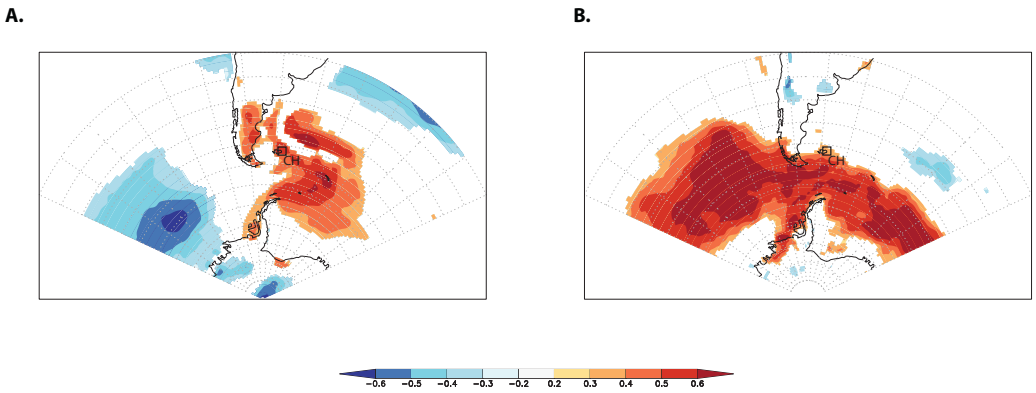

Figure 4: Correlation of relationship between the hemispherically-averaged Southern Annular Mode (SAM) index (Marshall, 2003) with 2-10 metre air temperature (Panel A.) and wind strength (Panel B.) in the ERA-79 Interim reanalysis (Dee et al., 2011) (July-June, 1979-2013). Location of Canopus Hill, (CH), Falkland Islands, shown. Analyses were made with KNMI Climate Explorer (van Oldenborgh and Burgers, 2005).

A.

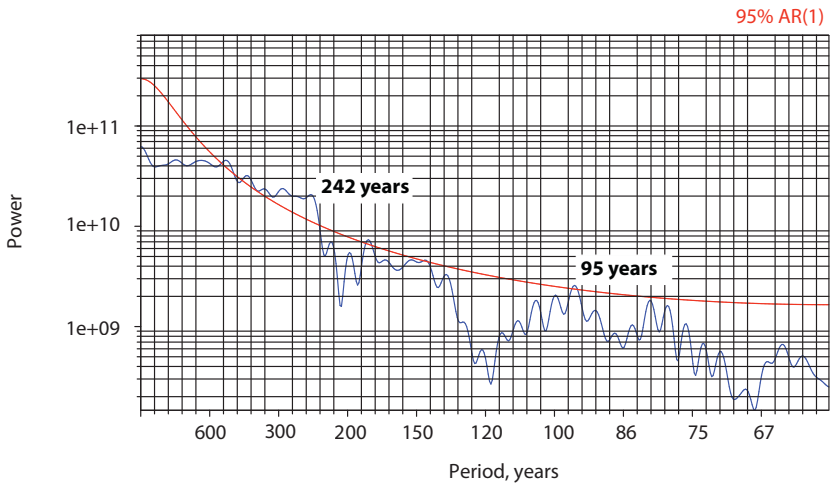
95% AR(1)
1e+11
1e+10
1e+09
Power
242 years
95 years
600
300
200
150
120
100
86
75
67
Period, years

B.

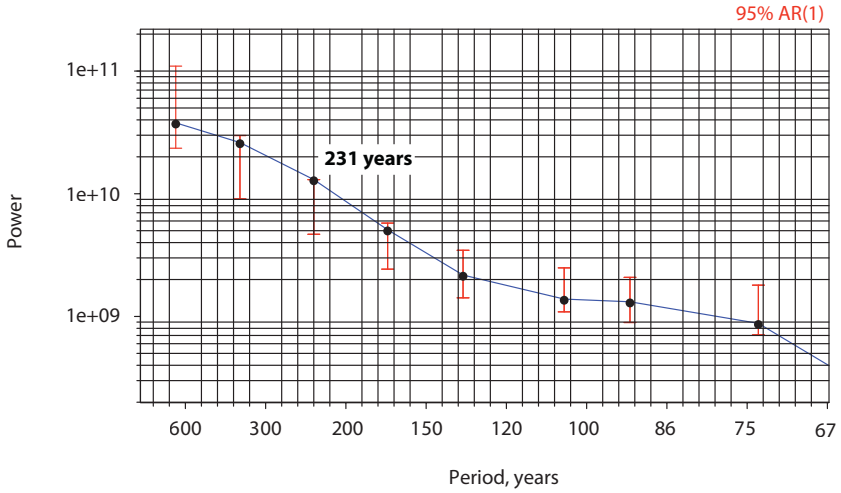
95% AR(1)
1e+11
1e+10
1e+09
Power
231 years
600
300
200
150
120
100
86
75
67
Period, years

C.

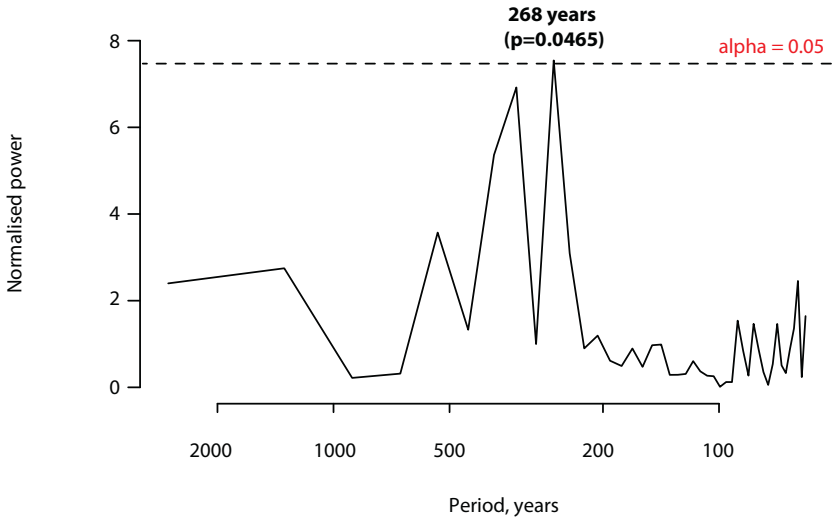
268 years
(p=0.0465)
alpha = 0.05
8
6
4
2
0
Normalised power
2000
1000
500
200
100
Period, years

Figure 5: Multi-Taper Method (MTM) (Panel A.), Monte-Carlo Single Spectrum Analysis (SSA) analyses (Panel B.) and Lomb-Scargle analysis (Panel C.) of charcoal from the Canopus Hill sequence. Error bars denote 95% confidence.

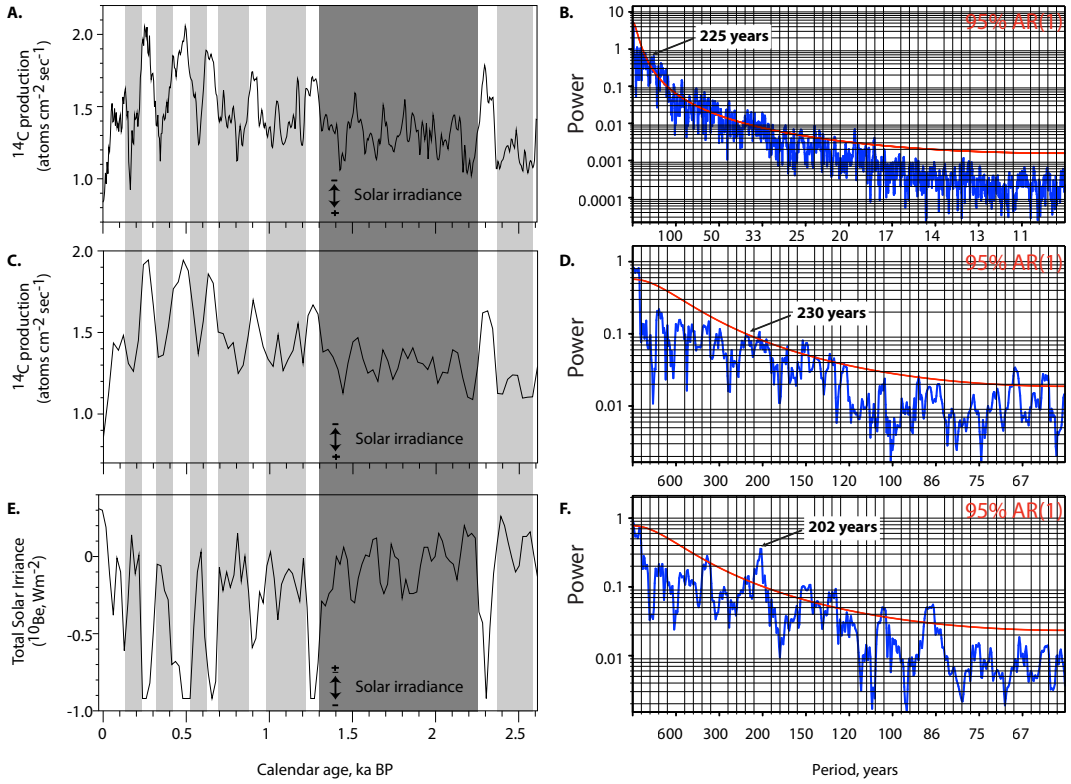

Figure 6: Changes in solar output and Multi-Taper Method (MTM) analysis of reconstructed radiocarbon (^{14}C) production rate (5-yr resolution; this study) (Bond et al., 2001; Turney et al., 2005) (Panels A. and B), ^{14}C production rate (resampled at 30 years) (Panels C. and D.) and Total Solar Irradiance (based on polar ice ^{10}Be) (resampled at 30-yrs) (Panels E. and F.) (Steinhilber et al., 2009) for the full length of each record. The dark gray column defines a millennial-duration period of sustained high solar irradiance in all records; the light gray columns define temporary (centennial-duration) periods of high irradiance. The periodicities that fall within the reported range of the de Vries cycle are identified in the MTM panels (200-230-yrs).

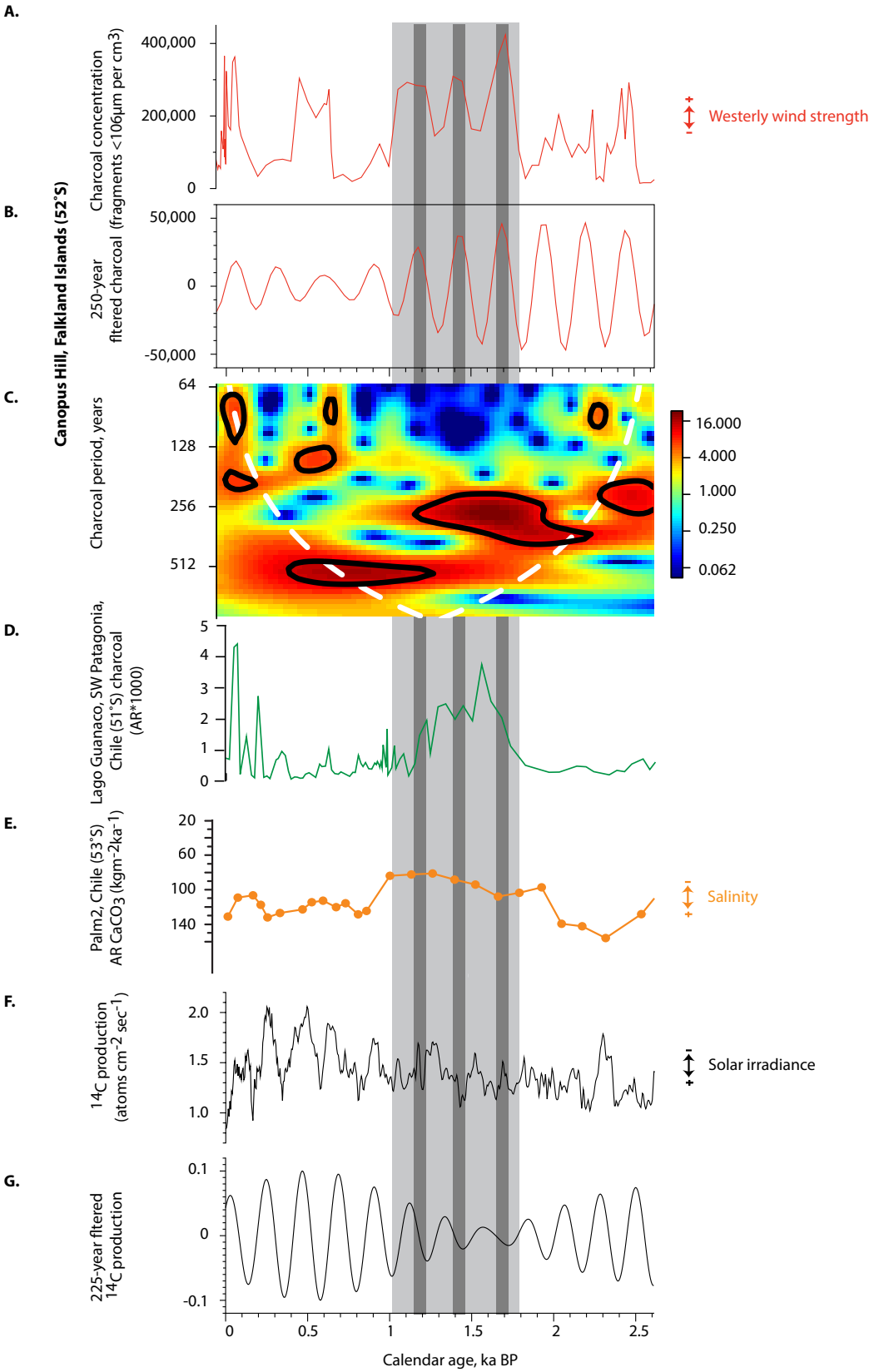
A.
B.
C.
D.
E.
F.
G.
Canopus Hill, Falkland Islands (52°S)
Charcoal concentration (fragments <106µm per cm3)
400,000
200,000
0
Westerly wind strength
250-year filtered charcoal
50,000
0
-50,000
Charcoal period, years
64
128
256
512
16.000
4.000
1.000
0.250
0.062
Lago Guanaco, SW Patagonia, Chile (51°S) charcoal (AR*1000)
5
4
3
2
1
0
Palm2, Chile (53°S) AR CaCO3 (kgm-2ka-1)
20
60
100
140
Salinity
14C production (atoms cm-2 sec-1)
2.0
1.5
1.0
Solar irradiance
225-year filtered 14C production
0.1
0
-0.1
0
0.5
1
1.5
2
2.5
Calendar age, ka BP

Figure 7: Charcoal concentration (<106μm) (Panel A.), Gaussian-filtered charcoal in the 250-year band (250±25 yr^{-1}) (Panel B.) and wavelet analysis of charcoal concentration (Panel C.) from Canopus Hill, Port Stanley Airport (52˚S). Solid black line in wavelet denotes 95% confidence in periodicity; white dashed line denotes cone of influence. Panel D. shows charcoal concentration data from Laguna Guanaco, Chile (51˚S) (Moreno et al., 2009) and Panel E. the biogenic carbonate accumulation rate (AR) from Palm2, Chile (53˚S) . Reconstructed ^{14}C production and Gaussian-filtered ^{14}C in the 225-year band (225±22.5 yr^{-1}) are plotted in Panels F and G. The light grey column defines the period of strong inferred westerly winds across the South Atlantic 2000 to 1000 cal. BP; the dark grey columns, peaks in charcoal 250-yr periodicity lagging minima in ^{14}C production rate (high solar irradiance).